IOPscience iopscience.iop.org

Home Search Collections Journals About Contact us My IOPscience

Surface modification of ferritic stainless steel by active screen plasma nitriding

This article has been downloaded from IOPscience. Please scroll down to see the full text article.

2012 J. Phys.: Conf. Ser. 379 012052

(http://iopscience.iop.org/1742-6596/379/1/012052)

View the table of contents for this issue, or go to the journal homepage for more

Download details:
IP Address: 106.190.212.235
The article was downloaded on 09/08/2012 at 22:48

Please note that terms and conditions apply.

Surface modification of ferritic stainless steel by active screen plasma nitriding

H Nii[1] and A Nishimoto[2]

[1] Graduate School of Science and Engineering, Kansai University
3-3-35 Yamate-cho, Suita, Osaka 564-8680, Japan
[2] Department of Chemistry and Materials Engineering, Kansai University
3-3-35 Yamate-cho, Suita, Osaka 564-8680, Japan

E-mail: akionisi@kansai-u.ac.jp

Abstract. Plasma nitriding is a surface modification process with a low environmental impact. Active screen plasma nitriding (ASPN) is one of the new plasma nitriding technologies, and can eliminate problems related to conventional direct current plasma nitriding (DCPN). In this study, ferritic stainless steel SUS430 samples were treated by ASPN to increase their wear resistance without decreasing their corrosion resistance. ASPN was performed in a nitrogen-hydrogen atmosphere with 25%N_2 + 75%H_2 for 18 ks at 623 K, 673 K, 723 K, 773 K, and 823 K under 600 Pa using an SUS304 screen. When the sample was treated at 673 K by ASPN, the pitting corrosion resistance and wear resistance of its surface were improved because of the formation of the S^{α} phase and a deposited layer containing Ni on the sample surface.

1. Introduction

Nitriding is a surface modification technique that is divided into three types according to the state of the activated nitrogen. These are gas nitriding, salt bath nitriding, and plasma nitriding. Of these three types, plasma nitriding, which is referred to as direct current plasma nitriding (DCPN), offers the following advantages: no environmental pollution, low gas and energy consumption, short treatment time, and high nitrogen potential [1,2]. However, this DCPN process produces a glow-discharge on the component surface, which can cause electrical problems such as the edge effect, hollow cathodic discharge, and arcing. This results in nonuniform properties such as hardness and thickness of the surface layer.

Active screen plasma nitriding (ASPN) offers a solution to these electrical problems. ASPN can eliminate electrical problems because the component is isolated electrically, and the glow-discharge is produced on a screen that is mounted around the isolated component [2-8]. This process can be used to treat ceramics and polymers [5,7].

Among metallic materials, stainless steel is widely used because of its high corrosion resistance. However, stainless steel has poor wear resistance because of its low hardness. Therefore, if stainless steel is applied to sliding parts such as gears and shafts, it is necessary to improve its hardness [9-11]. Most studies related to nitriding of stainless steel have dealt with austenitic stainless steel, but very few have focused on ferritic stainless steel. Ferritic stainless steels do not contain nickel and are inexpensive and eco-friendly materials.

Published under licence by IOP Publishing Ltd

In this study, the ferritic stainless steel sample SUS430 was nitrided by ASPN to increase its wear resistance without decreasing its corrosion resistance.

2. Experimental procedure

The sample material was a ferritic stainless steel SUS430. The chemical composition (mass%) of SUS430 is 16.13% Cr, 0.23% Ni, 0.82% Mn, 0.003% Si, 0.09% C, and the balance is Fe. The sample disk was 20 mm in diameter and 5 mm in thickness. The sample surface was mechanically ground with 150- to 1500-grid SiC, finely polished with a suspension of 0.05 μm alumina, degreased ultrasonically in acetone, and dried in air, before placing it into the nitriding furnace.

ASPN experiments were carried out using a direct-current (DC) plasma nitriding unit (NDK, Inc. Japan, JIN-1S). Figure 1 presents a schematic representation of the ASPN apparatus. A quartz (SiO_2) rod was placed on the cathodic stage in order to construct an isolated stage. The sample was placed on the sample stage and was isolated from the cathodic screen and the anode. The distance between the screen and sample was 10 mm. The screen material used was an austenitic stainless steel SUS304 in order to improve the corrosion resistance of the sample surface by Ni. The shape was an expanded metal mesh with a mesh size of 8 × 3 mm and a thickness of 0.5 mm, formed into a cylinder with a diameter of 77 mm and a height of 100 mm. The screen was thoroughly degreased ultrasonically in acetone and mounted on the cathodic stage around the sample stage.

Nitriding was performed in a nitrogen-hydrogen atmosphere with 25%N_2 + 75%H_2 for 18 ks at 623 K, 673 K, 723 K, 773 K, and 823 K under 600 Pa by the ASPN and DCPN processes. After placing the sample on the sample stage, the chamber was evacuated to ~3 Pa. Nitrogen and hydrogen were then introduced into the chamber and a DC bias voltage was applied, as shown in Table 1.

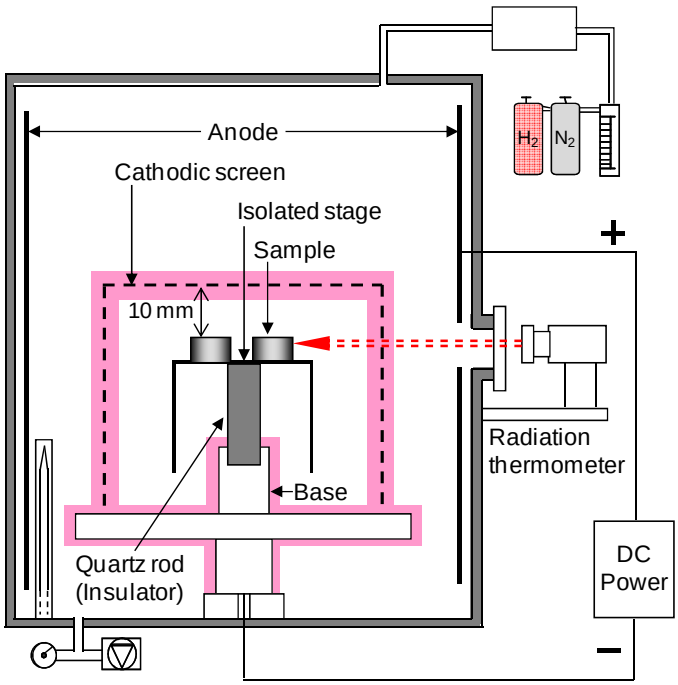


Figure 1. Schematic representation of the ASPN apparatus.

Table 1. Applied electric power of ASPN and DCPN process (W).

	623 K	673 K	723 K	773 K	823 K
ASPN	43	60	109	125	244
DCPN	64	88	150	240	355

After nitriding, the DC supply was switched off, and the sample was cooled to room temperature in the furnace. The nitriding temperature was monitored using a radiation thermometer, as depicted in Figure 1. Then, composition analyses of the sample surface were conducted using electron probe microanalysis (EPMA; JEOL, Japan, JXA-8800). The phase structures on the nitrided surface were determined using theta-2theta X-ray diffraction (XRD; RIGAKU, Japan, RINT-2550V). The entire top surface area of the nitrided samples was analyzed using XRD. Cross sections of each sample were first cut using a low-speed saw and then were polished and chemically etched. The nitrided microstructures of the surface and cross section were examined using an optical microscope and a scanning electron microscope (SEM; JEOL, Japan, JSM-6060LV). The hardness of the surface and the cross sections of the nitrided samples were measured using a Vickers microhardness tester (Matsuzawa, Japan, MXT50) under a load of 0.1 N. Five indentations were performed on each sample, and a 3-point average value (excluding both the maximum and minimum values) was used for the hardness. Wear testing was carried out at room temperature with a pin-on-disk tribometer. The conditions for wear testing were as follows: a running distance of up to 500 m, a wear load of 5 N, a rotation speed of 175 rpm, a wear radius of 6 mm, and a diameter of 6 mm for the alumina ball used for the counter material. After the wear test, the wear loss was calculated using the wear depth and the width of the wear track. A pitting corrosion test was carried out using a potentiostat. The sample was shielded by polytetrafluoroethylene (PTFE), exposing a 6 mm diameter area of the sample surface to the electrolyte. A 3.5 mass% NaCl aqueous solution was used as the electrolytic bath. DC polarization was performed potentiodynamically from -1.0 $V_{Ag/AgCl}$ to 1.5 $V_{Ag/AgCl}$. The anodic polarization curves were recorded at a sweep speed of 1.6 μV/s. On the basis of these polarization curves, the potential corresponding to a current of 1 A/m^2 was selected as the pitting potential.

3. Results and discussion

Figure 2 shows the appearance and EPMA line analysis of the treated sample surfaces. The DCPN sample has a non-uniform surface because of the edge effect. This edge effect occurs because of distortions of the electric field around the corners and edges of the sample, although the sample edge was well heated [12]. On the other hand, the ASPN sample had a uniform surface, and neither the edge effect nor arcing was observed. From the EPMA line analysis, the ASPN sample has a uniform nitrogen intensity distribution, but that of the DCPN sample differs between the edge and the center of the sample surface. In addition, nickel was detected on the ASPN sample. This indicates the presence of nickel from the screen material deposited on the ASPN sample surface.

Figure 3 shows an XRD pattern for the sample treated by ASPN and DCPN. While the phase of the sample surface treated by DCPN was different between the edge and center, the ASPN treated sample had a uniformly nitrided surface. When the sample was treated by ASPN, a γ'-Fe_4N phase was identified on the sample surface, unlike in the case of the DCPN sample. The nitriding mechanism in ASPN mainly involves the deposition and decomposition of activated clusters containing nitrogen and the metal elements of the cathodic screen [13-17]. Therefore, the γ'-Fe_4N phase was formed because of the high concentration of iron nitride, which was present on the screen.

In addition, the S^{α} phase, which is considered to be a supersaturated solid solution of nitrogen in the ferritic phase, was only observed when the sample was treated below 723 K [18]. When the sample was treated above 723 K, CrN was observed instead of the S^{α} phase. This indicates that the S^{α} phase decomposed into the α phase and CrN above 723 K. ($S^{\alpha} \rightarrow \alpha + CrN$)

Figure 4 shows SEM micrographs of the sample surfaces. On the DCPN sample surface, cauliflower-shaped particles were observed and the surface morphology was different at the edge and center. The surfaces of the ASPN samples have uniform and normal distributions of polygonal particles. It is believed that these correspond to Fe_xN particles from the screen material [13-17].

Figure 5 shows the cross-sectional microstructure of the nitrided samples. While the sample treated by DCPN has a non-uniform nitrided layer on its edge and center, the sample treated by ASPN has a

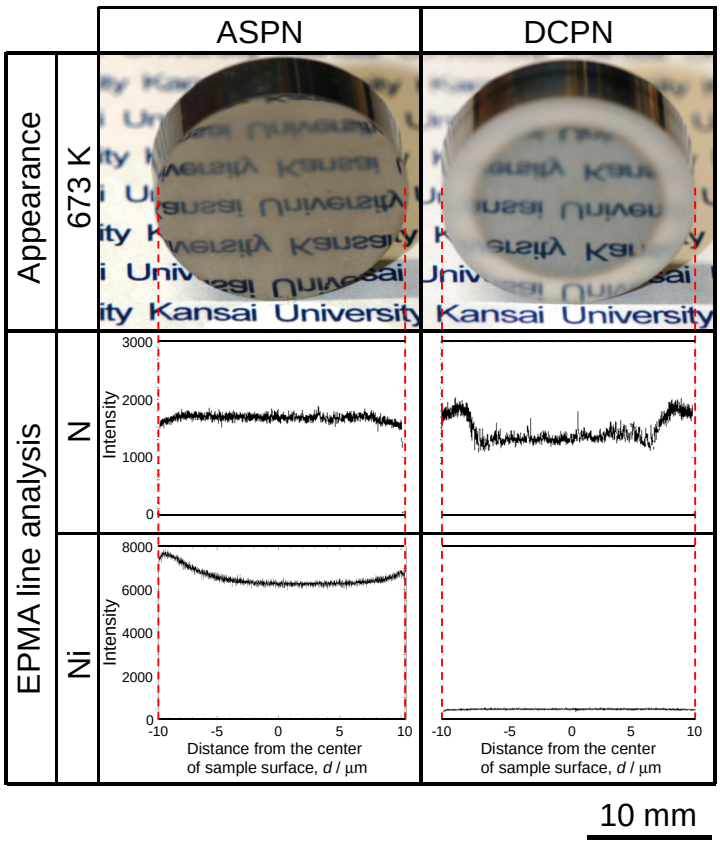


Figure 2. Appearance and EPMA line analysis of samples treated by ASPN and DCPN at 673 K.

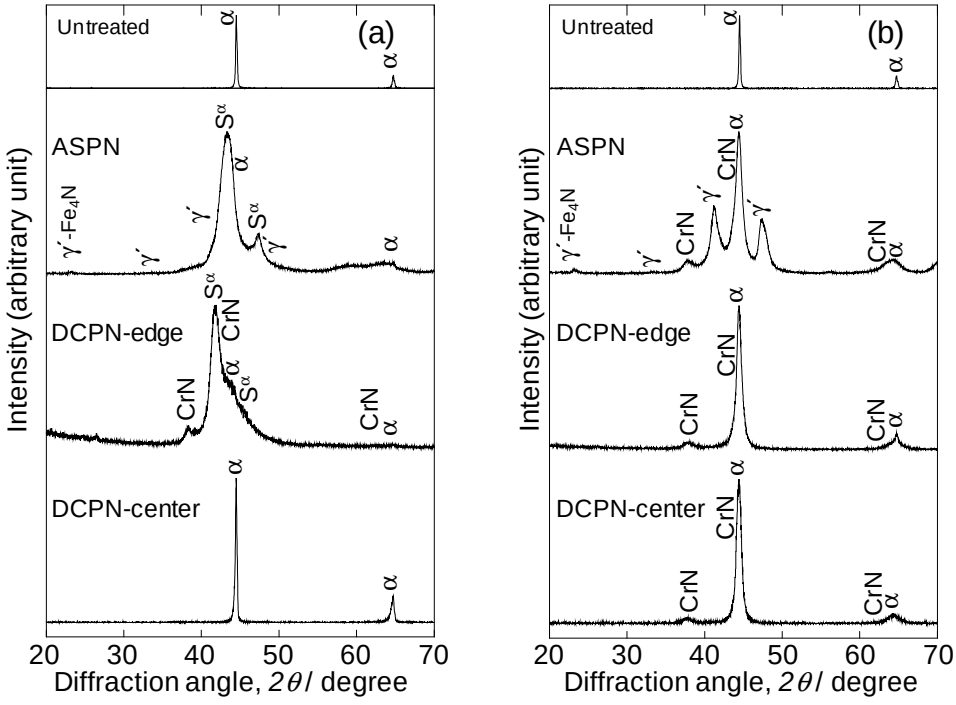


Figure 3. XRD patterns of untreated sample and samples treated at (a) 673 K and (b) 773 K.

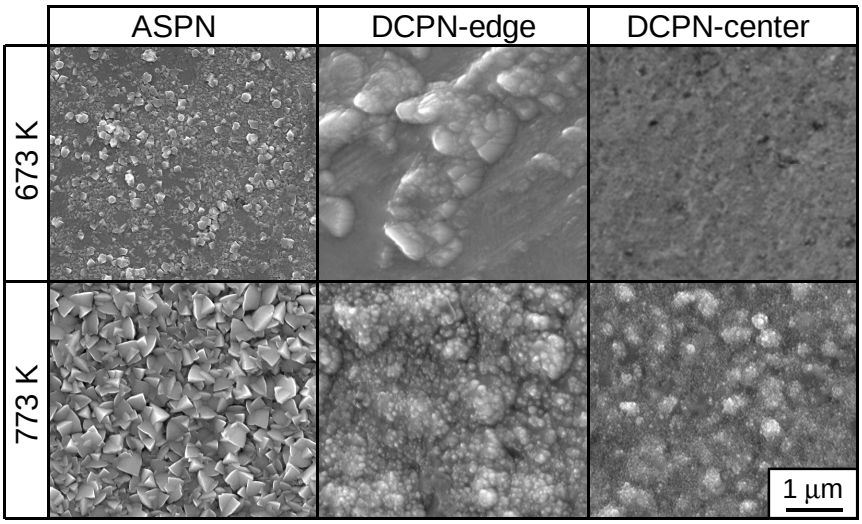


Figure 4. SEM micrographs of samples treated by ASPN and DCPN.

uniform nitrided layer. A white area near the surface was observed when the sample was treated at 673 K, and a black area near the surface was observed when the sample was treated at 773 K. The white area, which was not etched, is considered to be the S^{α} phase. On the other hand, the black area, which was highly etched, is due to the precipitation of CrN and a decrease in the chromium content of the ferritic stainless steel matrix.

Figure 6 shows the cross-sectional hardness distribution. The hardened areas corresponded to the white or black areas observed in the cross-sectional microstructure. The thickness of the hardened areas increased with increasing treatment temperature.

Figure 7 shows the results for wear loss for samples treated by ASPN and DCPN. With an increase in the nitriding temperature, the wear loss for each sample was less than that for the untreated sample. When the sample was treated above 723 K, the wear loss was very small. The decrease in the wear

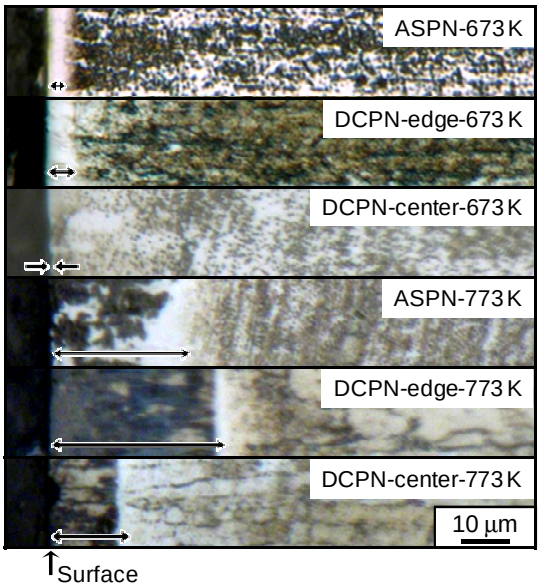


Figure 5. Cross-sectional microstructure of samples treated by ASPN and DCPN.

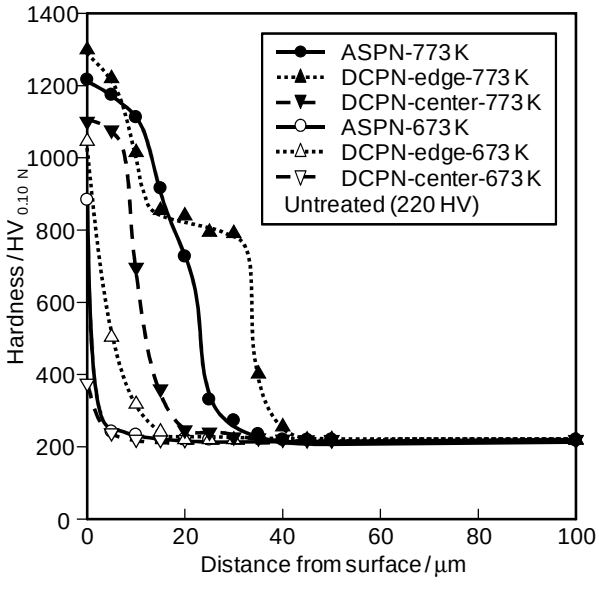


Figure 6. Cross-sectional hardness distribution for samples treated by ASPN and DCPN.

loss corresponds to the change of the surface hardness. Figure 8 shows the surface hardness for samples treated by ASPN and DCPN. With an increase in the nitriding temperature, the surface hardness increased because of either the formation of the S^{α} phase or the precipitation of CrN, as shown in Figure 3. This increase of the surface hardness resulted in a decreased wear loss.

Figure 9 shows the results for the pitting potential in a 3.5 mass% NaCl aqueous solution for samples treated by ASPN and DCPN. While the pitting potentials for DCPN samples were lower than that for the untreated sample (0.184 $V_{Ag/AgCl}$), those for the ASPN samples were higher than those for the untreated and DCPN samples. The ASPN samples have a thin layer on the surface, as shown in Figure 10. However, this thin layer was not observed at the edge and center of the DCPN samples. The layer produced by ASPN was about 200 nm thick, and contained Fe, Cr, Ni, and N. Therefore,

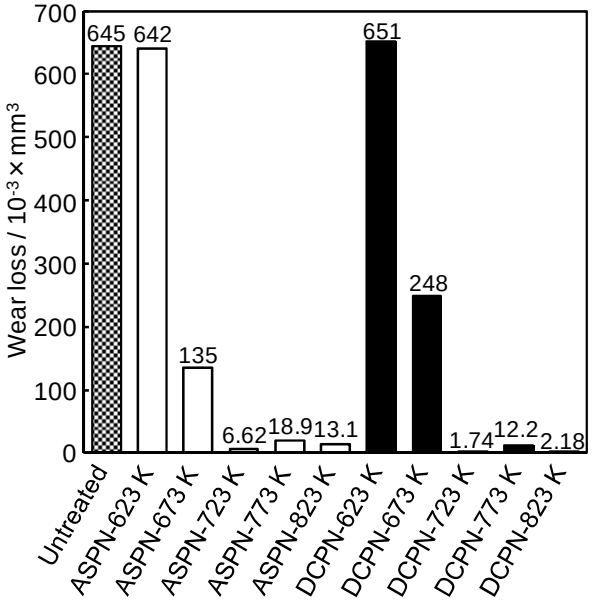


Figure 7. Wear loss for untreated sample and samples treated by ASPN and DCPN.

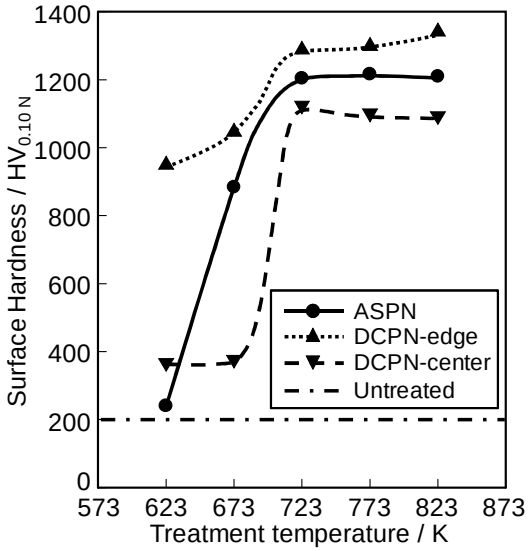


Figure 8. Surface hardness for samples treated by ASPN and DCPN.

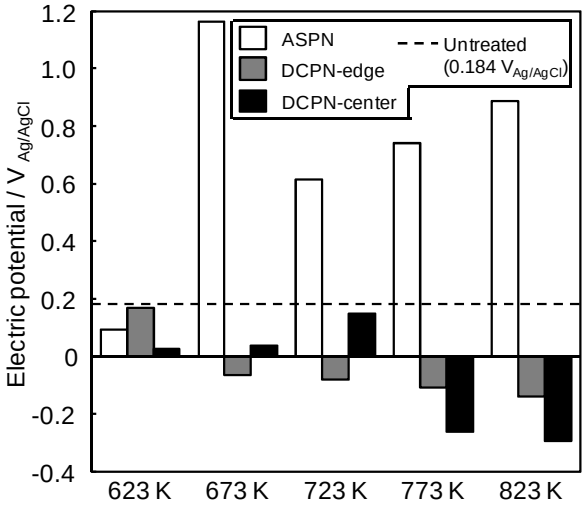


Figure 9. Pitting potential in 3.5 mass% NaCl aqueous solution for untreated sample and samples treated by ASPN and DCPN.

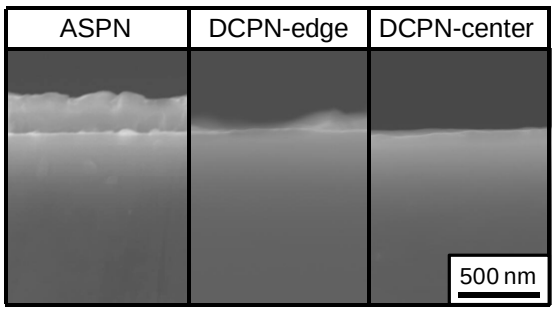


Figure 10. SEM micrographs of the cross section of samples treated by ASPN and DCPN at 673 K.

the layer was assumed to be a deposited layer of the screen material. The high pitting potentials of the ASPN samples were due to a layer containing Ni, which was coated on the sample surface. In particular, the ASPN sample treated at 673 K showed a high pitting potential. This indicates that the presence of the S^{α} phase under the deposited layer plays an important role for the pitting potential, because the corrosion resistance of the nitrided layer depends on the substrate [18].

4. Conclusions

Ferritic stainless steel SUS430 samples were nitrided by the ASPN process using an austenitic stainless steel SUS304 screen to improve their wear resistance without decreasing their corrosion resistance. Although samples treated by DCPN were found to have improved wear resistance, the pitting corrosion resistance values decreased and the nitrided layer was non-uniform. On the other hand, the sample treated at 673 K by ASPN had improved wear resistance, and the pitting corrosion resistance increased significantly because of the formation of the S^{α} phase and a deposited layer containing Ni on the sample surface.

References

[1] Sun Y and Bell T 1991 *Mater. Sci. Eng.* A **140** 419
[2] Nishimoto A, Nagatsuka K, Narita R, Nii H and Akamatsu K 2010 *Surf. Coat. Technol.* **205**(Suppl. 1) S365
[3] Li C X, Bell T and Dong H 2002 *Surf. Eng.* **18** 174
[4] Li C X and Bell T 2004 *Wear* **256** 1144
[5] Li C X and Bell T 2005 *J. Mater. Process. Technol.* **168** 219
[6] Ahangarani Sh, Mahboubi F and Sabour A R 2006 *Vaccum* **80** 1032
[7] Li C X, Dong H and Bell T 2006 J. *Mater. Sci.* **41** 6116
[8] Nishimoto A, Bell T E and Bell T 2010 *Surf. Eng.* **26** 74
[9] Dong H 2010 *Int. Mater. Rev.* **55** 65
[10] Nagatsuka K, Nishimoto A and Akamatsu K 2010 *Surf. Coat. Technol.* **205**(Suppl. 1) S295
[11] Kliauga M and Pohl M 1998 *Surf. Coat. Technol.* **98** 1205
[12] Alves Jr C, da Silva E F and Martinelli A E 2001 *Surf. Coat. Technol.* **139** 1
[13] Asahina S, Hosotani T and Kanayama N 2009 *J.Jpn. Soc. Heat Treat.* **49**(Spec. Iss.) 49
[14] Ahangarani Sh, Sabour A R and Mahboubi F 2007 *Appl. Surf. Sci.* **254** 1427
[15] Li C X 2010 *Surf. Eng.* **26** 135
[16] Zhao C, Li C X, Dong H and Bell T 2006 *Surf. Coat. Technol.* **201** 2320
[17] Li C X and Bell T 2003 *Heat. Treat. Met.* **30** 1
[18] Gontijo L C, Machado R, Casteletti L C, Kuri S E and Nascente P A P 2010 *Surf. Eng.* **26** 265